Am J Transl Res 2020;12(7):3792-3802
www.ajtr.org /ISSN:1943-8141/AJTR0103780

Original Article

A novel model of acute closed ventral spinal cord injury and its pathological changes in rats

Wei Hu[1], Ye Li[1], Lingzhi Zhang[2], Qingfeng Cai[1], Guanfu Wang[3], Xiaoming Hu[1]

[1]Department of Neurosurgery, Taizhou Hospital of Zhejiang Province Affiliated to Wenzhou Medical University, Taizhou 317000, China; [2]Department of Hospital Infection, Taizhou Hospital of Zhejiang Province Affiliated to Wenzhou Medical University, Taizhou 317000, China; [3]Department of Urinary Surgery, Taizhou Hospital of Zhejiang Province Affiliated to Wenzhou Medical University, Taizhou 317000, China

Received October 20, 2019; Accepted May 31, 2020; Epub July 15, 2020; Published July 30, 2020

Abstract: Objective: To establish a spinal cord injury (SCI) model by ventral violence and explore its pathological changes. Methods: We first designed and made a shape-suitable impinger. SD rats were divided into 4 groups according to force momentum calculated by weight and height: Group A (350 g*28 cm), Group B (280 g*28 cm), Group C (210 g*28 cm), and Group D (sham, 0 g*0 cm). Then the anterior border of the rat's T11 centrum was hit by the by impinger via a free-falling method. Locomotor functional (Basso, Beattie and Bresnahan scale-BBB scale), GFAP expression and pathological changes, complications, and mortality were observed. Results: The BBB scale scores were significantly different among all groups. Contusion, hematoma, and subarachnoid hemorrhage appeared at 1-6 h after injury in group A and B. Edema was obvious and the inflammatory cell infiltrated at the time of 6-48 h. Cicatricial contracture and porosis formed at 3-4 weeks, while group C only showed sporadic punctate hemorrhage. GFAP expression changed by time and location dynamically compared with group D. Various complications appeared in the experimental groups. Intestinal obstruction was the main cause of death. The mortality was significantly different among the groups ($P<0.05$). Conclusion: The acute ventral closing SCI model could be set up successfully by a shape-suitable impinger. The procedure was simple and repetitive. Neural function deficiency, pathological changes, and mortality were consistent with the injury controlled by coup momentum. Under the condition of this model, astrocytes went through an acute damage period and continued in the further hyperplasia stage.

Keywords: Animal model, acute closed ventral spinal cord injury, impinger, pathology, neurologic diseases

Introduction

In high-speed transportation and extreme sports, the incidence of spinal cord injury (SCI) is very high [1]. Currently, although the incidence of SCI has been increasing, its pathological mechanism was complicated and remain unknown, and there are few previous studies on it. However, whatever the level of violence, most SCI incidents are caused by buckling, axial or shear force, leading to compression fractures, burst fractures or chance fractures, and resulted in various kinds of SCI under a sober state, part of these cases belonging to acute ventral closing SCI.

Many previous studies have confirmed that neuronal injuries, such as necrosis and apoptosis in secondary spinal cord and neuron injury, have an intrinsic role on the function of locomotion, sensory, and autonomic nerve system. Therefore, neuronal research of SCI was very important. It is also very important to understand the mechanism of SCI clearly in order to find effective treatment methods.

Currently, there are no suitable animal models that can imitate the pathologic change of SCZI [2]. Therefore, it is important to set up an ideal animal model of SCI. Although various SCI models had been reported, such as crosscut injury, oppressed injury, contusion injury, photochemistry injury, and ischemia-reperfusion injury model [3], these models represent different styles of SCI. In clinical practice, partial SCI were caused by ventral violence while the vertebral canal closed but this kind of model couldn't be established in animals until now. Some investigators have successively set up opening SCI models by ventral force [4]. However, the

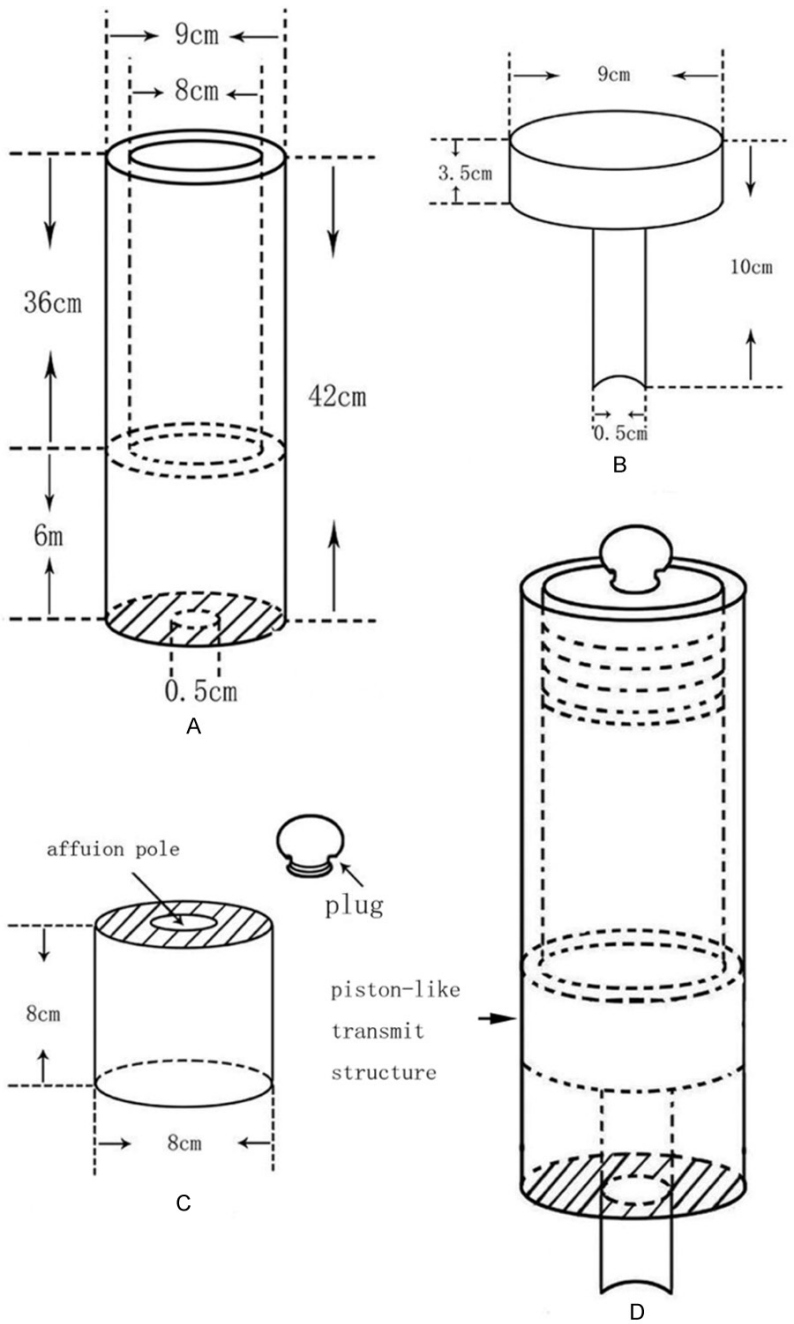

Figure 1. Shape-suitable impinger. This figure shows each part of the self-designed impinger and the fabricated device. A. Orbit; B. Transmissible rod; C. Adjustable weight; D. Fabricated device. The orbit was a circular plastic cannula with a smooth inside wall, adjustable weight is made up of a capacity bottle and bottle plug, and a transmissible rod is made up of a piston end and shape-suitable tip. The quality of the adjustable weight could be adjusted randomly to precisely guarantee momentum regulation. The upside of the Orbit's inside wall was smooth and coincided to the adjustable weight and the inferior part of the orbit constraint the piston end and formed the piston-like transmit structure. The front-end of the shape-suitable tip is long and narrow and its inward arc shape is similar to the shape of the spinal ventral side and then adjusted to fit it, thereby reducing the aortic injury and ensuring the well-distributed forces on both sides. These guaranteed the unity of momentum and direction of each model.

acute ventral closing SCI model was not reported presently. Hence, we made this model without opening the vertebral canal and adopted an instantaneous violent manner under the basal anesthesia and explored the neural function deficiency and pathological changes in order to provide a suitable animal model for medical research on SCI. Considering the above-mentioned reasons and the complexity of neuronal pathological changes after SCI, Neuronal counting and apoptosis detection are difficult to reflect neuronal changes as a whole after SCI. We also explored neuronal pathological changes at different sites and times by morphological observation stained with H&E and Nissl body to comprehend the course of neuronal degeneration and death generally. To the best of our knowledge, our model is the first acute closing ventral SCI model caused by a shape-suitable impinger.

Materials and methods

Materials

Design of the shape-suitable impinger: The shape-suitable impinger consisted of an orbit, adjustable weight transmission rod (**Figure 1**). This controllable force centrum machinery performed the SCI model.

Experimental animals: Ninety-two healthy SD adult rats, weighting 220 g-250 g was provided by the experimental animal center of Zhengzhou University. The protocol of this experiment followed the regulations of

the ethical committee for animal research of the Zhengzhou University.

Reagents and instruments: The reagents and instruments included Midazolam (5 mg/ampoule), HE kit (Bi Yun-tian biotechnology research institute), and an Immunofluorescence Microscope (OLYMPUS).

Midazolam was adopted as an anesthetic characterized by less irritation, rapid revival, and less influence on the breath and cardiovascular system [5], while rapidly contributing to an inferior sober state and alleviating psychological stress and stress reaction. Midazolam effects would create the injury condition closer to the real situation in a clinical setting when subjected to an external force. This procedure was both ethical and clinical.

Experimental design

Establishment of the animal modeling: The rats were divided into four groups according to force momentum calculated by weight and height. Experimental group: group A (350 g×28 cm), group B (280 g×28 cm), group C (210 g×28 cm): Control group: group D (sham, 0 g×0 cm).

The rats were restricted from food for 12 hours to empty their stomach and water intake was stopped 3 hours prior to the surgery. Midazolam anesthesia was administrated by intraperitoneal injection (0.5 mg per kg body weight). The rats were fixed in a dorsal position and the four limbs were stretched under the inferior sober state. The T-10 centrum was suspended in mid-air and then the internal organs were pushed away by the drive rod. The tips stick to the T-11 centrum closely and attack the piston end by the vertical falling of the force momentum. The rats demonstrated spasmodic twitching of the tail and both lower extremities after injury and lost partial or complete motor function of both lower extremities. The rats that regained consciousness without dying within 48 hours were considered to be the successfully established model. Group D underwent sham surgery without attacking the drive rod. There were 26 rats in groups A and B and 18 rats in groups C and D. After the surgery, each rat was placed in a single cage and food-intake was restricted to 1/10 of the body weight. The abdomen of the rat was gently massaged to assist defecation. The rats were also injected with 3 ml of 10% glucose via vena dorsalis penis 3 times a week.

Motor function evaluation: Five rats in each group were randomly picked for the neurological evaluation. The motor functional test was performed at d1, d7, d10, d14, d21, d28 postoperatively using a double-blind method. Based on the three independent tests, neurologic function was recorded according to the BBB (Basso, Beattie and Bresnahan) scale and averaged.

Morphology and pathology: Two rats in each group at 1 h, 6 h, 48 h, 7 d, 28 d intervals underwent heart perfusion fixation with 4% of paraformaldehyde and they were fixed overnight, prepared for histology (20 μm thick sections), and observed by an H&E and cresyl violet stain. The specimens were divided into three segments: 0.20 cm surrounding the main injury region (center injury segment -CIS), 0.20-0.50 cm region at a distance from the injury region (near injury segment -NIS), and a 0.50-0.80 cm region from the injury region (far injury segment -FIS).

Criteria of neuronal change: The criteria of morphological change were according to those reported in the literature [6]. The hub of the injury segment was set as zero, we then measured the length of the spinal cord that contained the degenerative neuron along the macro axis and performed three times in each slice and averaged the results.

Immunohistochemistry: The GFAP expression was performed at 1 and 6 hours and 2 and 7 and 28 days after the injury by the immunohistochemical SP (streptavidin-perosidase) method in group B and D. All of the procedures followed the manufacturer's instructions. The sections were observed under the microscope and 4 fields were selected under low power (100×) and 10 photographs were taken under high power (400×). The images were analyzed by Image-pro plus 6.0 software. We measured the mean optical density (MOD) and positive area (%) of per field respectively and applied relative content (RC = MOD* positive area %) to represent the positive component.

Complication and death: We excluded the perfused rats and observed the complications from d2 to d28 and the death situation from d1 to d28. The complications that were observed included urine retention, hematuria, urinary tract infection, pulmonary infection, edema of affected extremity, pressure sore, self-mutila-

Table 1. Comparison of BBB score

Group	1 d	7 d	10 d	14 d	21 d	28 d
A	0.93±1.44	3.53±1.99	4.66±2.38	7.33±2.47	9.87±2.47	11.27±2.69
B	2±3.53#	3.4±2.13#	4.20±2.62#	10.40±3.18*	13.87±2.90*	13.27±2.89*
C	4.40±4.24	17.93±2.81	18.53±1.60	19.87±1.13	19.60±1.30	19.87±1.19
D	19.87±1.36	20±1.07	19.87±1.13	19.93±1.10	20.47±0.64	20.60±0.74

Note: versus group A: #P>0.05, *P<0.05.

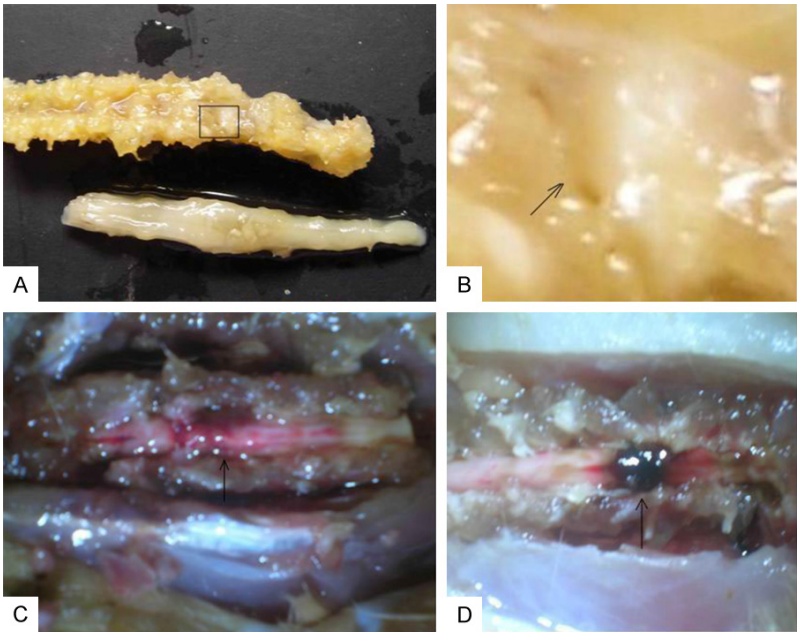

Figure 2. Gross appearance of spinal cord injury. (A) Vertebral fracture and spinal cord injury shown at the same level; (B) Enlarged view of the fracture line in picture (A), vertebral fracture line could be seen clearly (arrow); (C, D) Open vertebral canal at 6 h after the injury, subarachnoid hemorrhage, contusion, and hematoma could be seen clearly (arrow).

tion, mutual mutilation, and intestinal obstruction.

Statistics analysis

SPSS13.0 software was used for the statistical analysis. All data were presented as Mean ± S.D. A chi-square test was used to analyze the significant difference of the rate of sample among the groups. The BBB scale scores of all animals in the same experimental group in the same interval were averaged and the statistical analysis of these scores was performed using repeated measures analysis of variance (ANOVA) and a pairwise multiple post hoc comparison using the Bonferroni *t*-test. One-way ANOVA was used to compare means in one interval among the groups and a *t*-test was used for significant difference analysis of two means between the groups, α (size of test) = 0.05.

Results

Motor function

The rats in group D walked normally. The rats in group C returned to normal at 7 d after the injury. The scores of group A and B showed an increasing tendency after SCI. They demonstrated complete flaccid paralysis of the hind limbs immediately after injury and relatively partial recovery in light activity during 5-7 d. More obvious recovery presented at d14, but the rats could not support their whole body after 4 weeks. Repeated measures analysis of variance showed a significant difference between each group (P<0.05) (**Table 1**).

Pathological changes

Gross appearance: As shown in **Figure 2**, a fracture of the centrum was found in a few samples. Contusion, hematoma, and subarachnoid hemorrhage were observed within 6 h after injury. Most injured lesions became swollen at 6 h and subsided after 7 days. After 3-4 weeks, the injured region became analosis, while thinning the surrounding tissue. The changes described above were not found in group C.

Histology changes

As **Figure 3** shows, the sections stained with HE showed the following histopathological

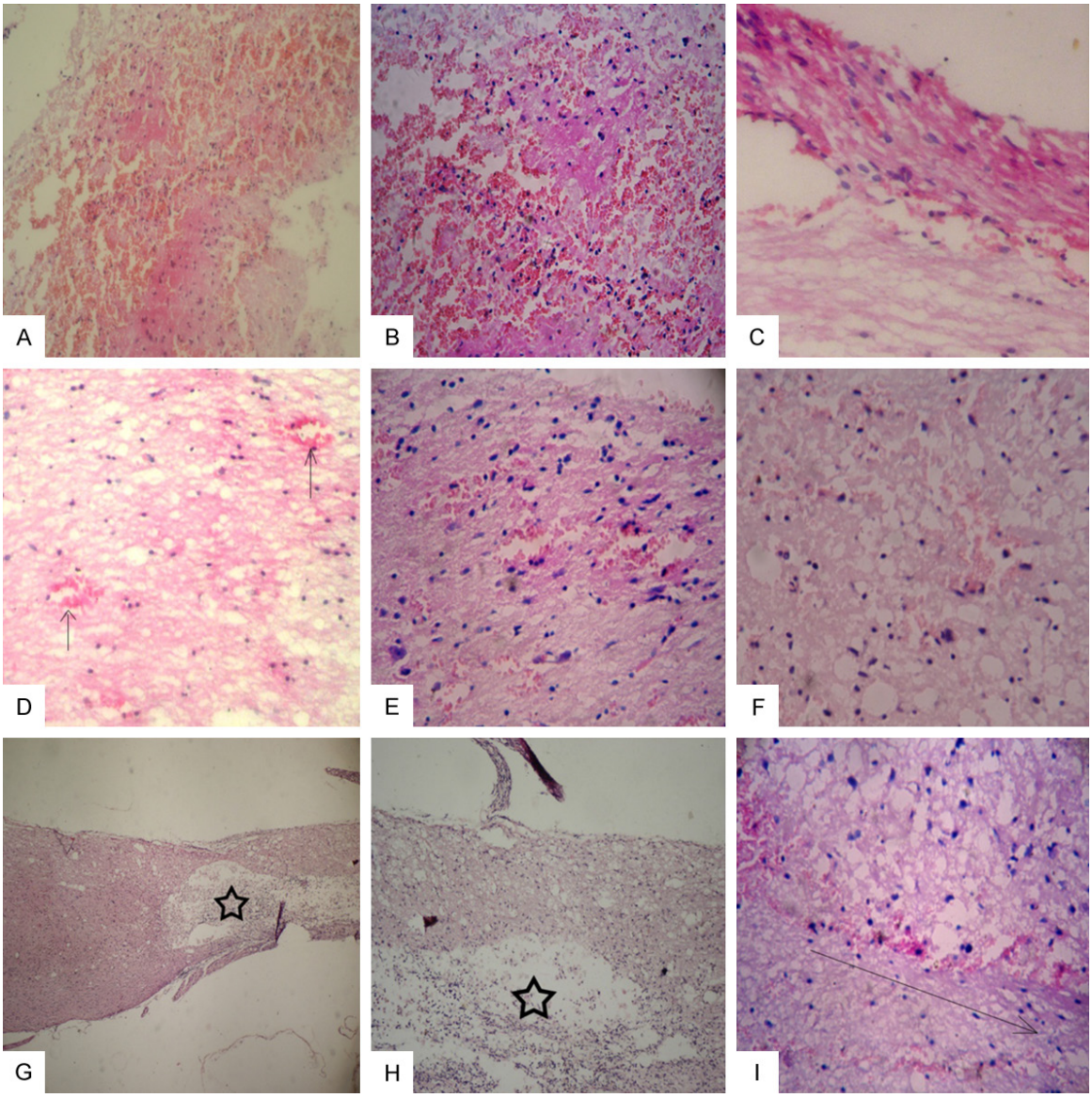

Figure 3. General pathological observation of spinal cord injury. A-C. 1 h to 6 h after the injury in group A and B, hematoma, contusion, and subarachnoid hemorrhage was shown in group A, B. (HE, original magnification ×100, ×200, ×400); D. 6 h after injury, typical pathological change of group C (arrow): small hemorrhagic lesion. (HE, original magnification ×100); E. 1 h to 6 h after injury, the tissue space was normal and edema was not obvious. (HE, original magnification ×400); F. 6 h to 48 h after injury, the tissue space near the contusion and hematoma expanded, indicating edema occurred obviously, with the mononuclear inflammatory cell infiltrated abundantly. (HE, original magnification ×200); G, H. 4 weeks after injury, cicatricial constriction and cavitas formed at the injury site (asterisk), (HE, original magnification ×40, ×100); I. 6 h after injury, multiple contusions could be seen in the gray matter of the cephal and caudal end of the force spot along the axis of ordinates (arrow), (HE, original magnification ×200).

changes: 1-6 h after injury: hematoma, contusion, subarachnoid hemorrhage in group A and B (**Figure 3A-C**), only dispersed punctate hemorrhage showed in Group C (**Figure 3D**), and no abnormalities in group D. The tissue space was still normal, and the interstitial edema was not obvious (**Figure 3E**). 6-48 h later, the hematoma and tissue space expanded, and large number of inflammatory cells were infiltrated (**Figure 3F**). Enlarged tissue space was not obvious at 7 d. Cicatricial constriction and porosis formed at 3-4 week (**Figure 3G**, **3H**). Posttraumatic hematoma and contusion were located mainly in a coup position, while extensive small lesions were found in the cephal-caudal end of the grey matter along the long axis of the spinal cord in

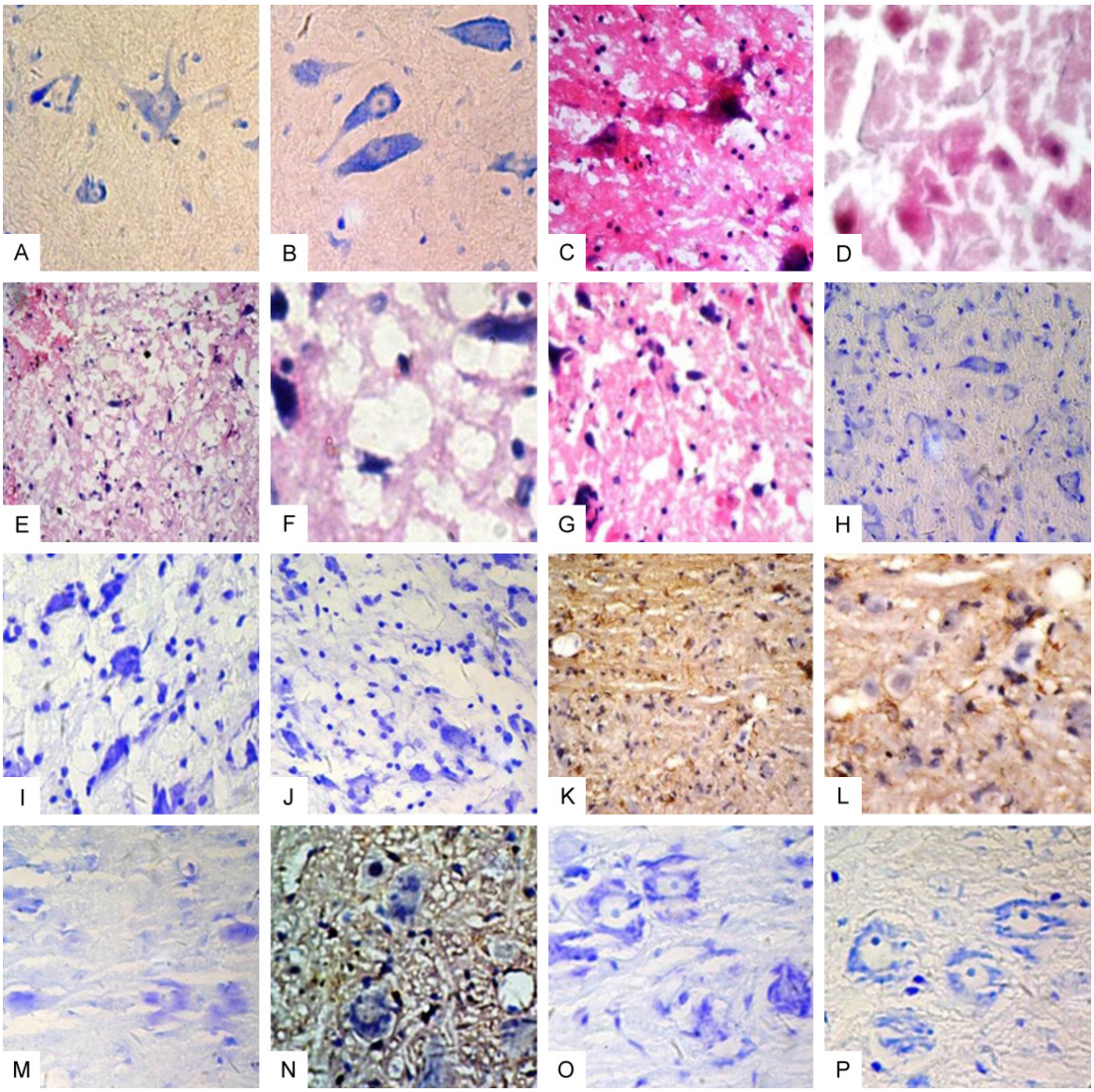

Figure 4. Morphological change of the degenerative neuron. (A, B) Neuron in group C. Group D was normal control; (C-G) Within 48 h after injury in group A and B, neuronal debris and red neuron appeared to be located in the injury segment (C, D) neuronophagia and karyopycnosis located in near injury segment (E-G), most included an irreversible injury; (H-J) ischemic neural degeneration such as neuronophagia and ghost cell, apoptotic body were found near the injury segment at 1 week; (K-M) ischemical neuronal degeneration such as vacuole structure and homogeneous change were visible in the near injury segment at 4 weeks, these were mostly irreversible injuries. Around the degenerative neuron, the GFAP expression was high; (N-P) neural apoptosis and central chromatinolysis were found either near the injury or far from the injury section.

group A and B (**Figure 3I**). However, different distributions appeared in group A and B. Group A had lesions both in NIS and FIS, only NIS had small contund foci while presenting hemorrhagic spots in FIS.

Morphological change of the neuron

Observed by optical microscope, neuronal injury occurred in group A and B, including irreversible injury, reversible injury (**Figure 4**) or combined in some cases.

Expression of GFAP

The expression of GFAP at 1 h and 6 h and 2 h and 7 h and 28 d in group B and D was determined by immunohistochemistry. The GFAP expression presented in a pattern in group D (**Figure 5A**, **5B**), as seen in **Table 2** and **Fig-**

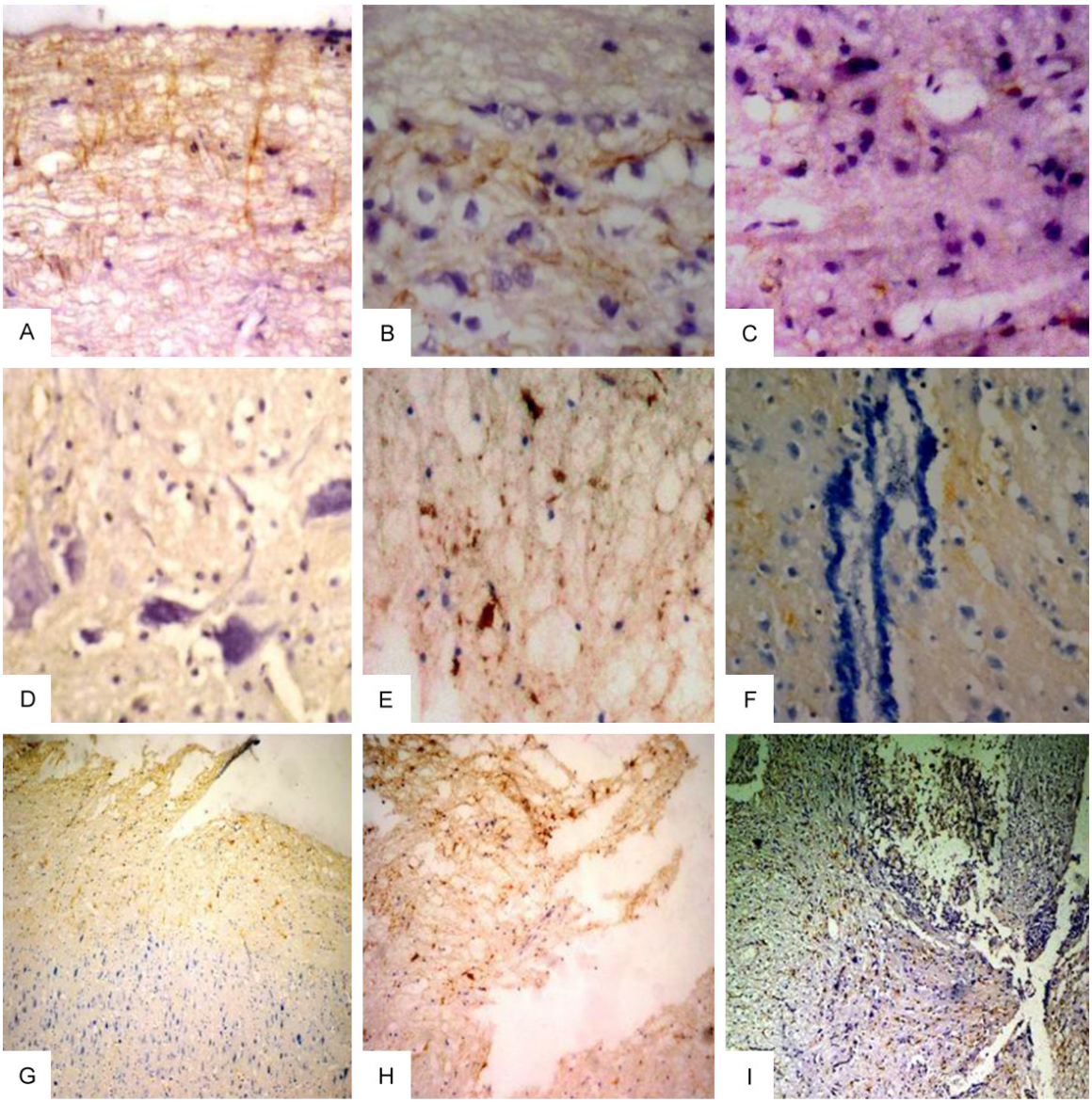

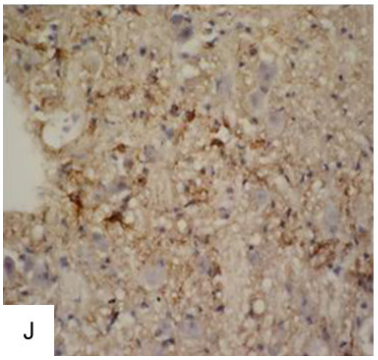

Figure 5. The expression of GFAP in the rat's spinal cord. A, B. The expression of GFAP in a normal spinal cord. The positive area was close to the junction of the spinal pia mater and grey matter. There was a low expression in the gray matter, (SP, original magnification ×100, ×200); C, D. A decreased GFAP expression in white matter and minimal expression in gray matter at 1 hour after the injury in group B. (SP, original magnification ×400, ×400). E-H. 6 hours later, the GFAP expression appeared and enhanced in the white matter near the injured region, pia mater spinalis, and grey matter near the central tunnel. (SP, original magnification ×100, ×400, ×100, ×400,). I. Axial view, positive cells of GFAP mainly located near the injured segment at 7 days. (SP, original magnification ×100). J. Both white and gray matter had higher expressions of GFAP at 28 days after injury. (SP, original magnification ×200).

ures 5, **6**. In group B, there was minimal GFAP expression in the gray matter and a decreased expression in the white matter 1 h after injury (**Figure 5C**, **5D**). 6 hours later, the GFAP expression increased at pia mater spinalis near the injured region and grey matter near the central tunnel (**Figure 5E-H**). The expression of GFAP continued to increase especially in the far segment of the injured area at 48 hours after injury and located mainly in near the injured segment

Table 2. Expression of GFAP in normal spinal cord and group B

		RC value				
		1 h	6 h	48 h	7 d	28 d
B	N-W	34.87±5.56※	37.06±5.44※	43.33±4.40★,○	64.84±10.38※,○	95.40±20.62※,○
	N-G	2.84±0.78△	4.49±1.28△	12.05±1.50★	24.33±5.71△	51.48±5.84△
	F-W	35.69±5.75※	36.07±5.93※	54.78±6.85※	59.74±3.99※	68.81±8.42※
	F-G	6.71±2.04△	4.04±0.97△	17.93±2.86△	19.05±1.44△	22.62±3.55△
D	W	44.37±5.26	43.23±5.88	44.59±5.18	42.12±3.89	47.87±3.00
	G	12.02±3.12	13.49±4.41	12.95±2.19	11.41±1.92	12.43±2.36

Note: (1) N = near injury segment, F = far injury segment, W = white matter, G = gray matter, B = group B, D = group D. (2) versus group D-W: ※$P<0.05$, ★$P>0.05$; versus group D-G: △$P<0.05$, ★$P>0.05$; versus group B-FW: ○$P<0.05$.

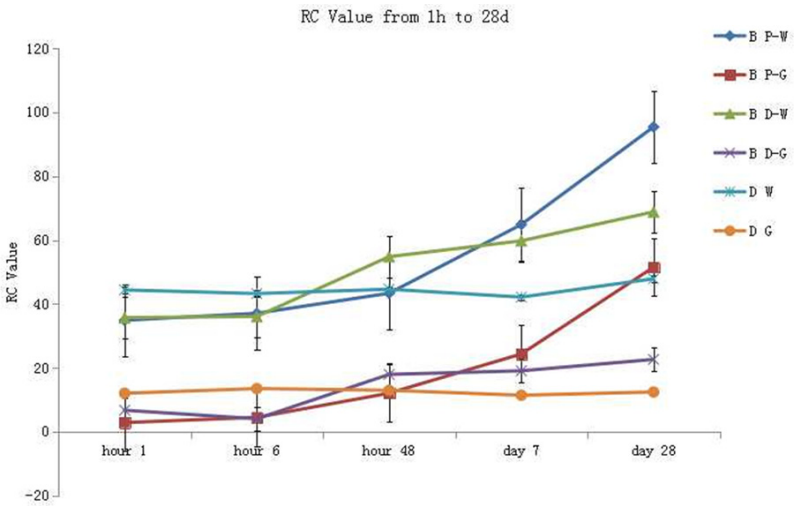

Figure 6. Comparison of the RC Value of GFAP in a normal spinal cord and group B. The relative content value (RC value = mean optical density × positive area, %) represented the positive component of GFAP expression at 1 h, 6 h, 2 d, 7 d, and 28 d intervals after injury in group B. Compared to group D, there was a significant decline at 1 h and 6 h and a significant increase at 7 d and 28 d (P<0.05; paired t-test). The GFAP expression increased at 1 h and 6 h and then increased after 6 h and was mainly located in the far injury segment at 48 h. Furthermore, the main expression area transferred to the near injury segment at 7 d to 28 d. There was a gradual increase tendency of the RC Value from 1 h to 28 d. Note: N = near injury segment, F = far injury segment, W = white matter, G = gray matter, B = group B, D = group D.

Table 3. Mortality comparison between group A and B

Group	N	Dead	Survival	Mortality (%)	X^2	P
A	16	5	11	31.25	8.00	0.018
B	16	1	15	6.25		
C	16	0	16	0		

at 7 days and the positive expression of GFAP developed from the local region to the hol-region around the injured area at 7 days (**Figure 5I**). Both white and gray matter had a higher expression of GFAP at 28 days after injury (**Figure 5J**). There was a striking decline in the RC Value at 1 h and 6 h intervals and a distinguished increase in the RC Value at 7 d and 28 d intervals (versus group D, $P<0.05$; t-test) and showed a gradual improvement in the RC Value from 1 h to 28 d (**Table 2**; **Figure 6**).

Complications and mortality

30 rats underwent a pathological examination and 40 rats' complications and mortality were observed after the operation. During d2 and d28, 8 rats died in group A and B and 0 in group C and D. 3 rats died from bladder rupture, intestinal obstruction, hematuria, and pulmonary infection respectively during days 2-7. 3 rats died from days 8-14 post injury because of an intestinal obstruction. 2 rats died from day 15 to day 28 as the result of vesical rupture due to the inappropriate massaging of the bladder. Complication and death at d2 to d28 were shown in **Table 3**. There was a difference of mortality among groups in d2 to d28 (reject 2 because of human factors) ($P<0.05$, Chi-square test).

Discussion

Ventral violence could case abdominal organ injuries, which make it difficult to establish an animal model of this injury. We found an ana-

tomic space between the diaphragm and liver, which doesn't have important organs except for the aorta from the view of anatomical analysis. At the horizontal plane of this gap, while pushing the skin to the spinal column and avoiding squeezing the surrounding organs, the violence could transfer to the spinal cord through the shape-suitable impinger (**Figure 1**). By using this unique machinery, we established this model with good repetitiveness and that is well regulated in a simple procedure.

We also explored the neural functional cahnges (**Table 2**). There was a significant difference not only between the experimental group and the control group but also among the experimental groups ($P<0.05$). It also demonstrated that this method could successfully cause SCI and the regulated degree of SCI resulted in the corresponding neural function deficiency. Furthermore, the primary injury of hematoma, contusion, subarachnoid hemorrhage, and secondary changes such as inflammatory cell infiltration, edema, cicatricial contracture, and porosis were observed in this model, indicating that it could reflect the pathological changes of SCI and is consistent with other reports [6]. The distinctive distribution of the lesions in group A and B and punctuate hemorrhage found in group C were also observed. In **Table 3**, the analysis of mortality among the groups had been continued and the mortality had a significant difference, showing that the quality of coup momentum could cause different mortality rates. Changes of neural function, pathology, and mortality had consistency to the coup momentum in our experiment.

Many research studies have focused on the decreased number of neurons in SCI at an earlier time, while some scholars indicated that there was no significant reduction of neurons after SCI [7]. In recent years, some researchers considered that apoptosis could occur in the injured spinal cord [8]. Apoptosis, nowadays, could be identified by the morphological criteria mentioned above and the prevalent biochemical criteria. Although TUNEL and ISEL had been applied to neuronal apoptosis research extensively, as long as DNA-cracking appeared in apoptosis, necrosis, and autolytic cell death, the quantity of 3'-OH terminal would increase thereafter. So, TUNEL and ISEL reflect nothing but the possibility of apoptosis [9].

Polymorphous neuronal degeneration was found in the rat's spinal cord after injury. 1 h to 48 h after injury, due to the spillover of cytoplasm, rupture and resolution of the hemocyte and aggravation of the inflammatory reaction occurred [10-12]. Afterwards, the ischemic scope enlarged gradually, and most were irreversible injuries including cytoclasis, karyopycnosis, red neuron, etc. The range of neuronal injury did not enlarge conspicuously at 1 week and karyopycnosis, ghost cell, and neuronophagia existed near the injury segment. Neural apoptosis could be seen sporadically, the appearance of ghost cell hint that ischemic neuronal injury caused more aggravation at this point in time. During 48 h to 1 week, the range of injury did not enlarge conspicuously, which illustrated that the degree of neural injury peaked within 48 h after injury [13]. It is suggested that an inflammatory reaction could cause a secondary injury of the spinal cord with necrotic tissue clearing and renovation [14, 15].

Nevertheless, the range of neuronal injury enlarged conspicuously at 4 weeks. Ischemic changes of the end-stage, such as vacuole structure and neural homogeneous change existed in NIS and central chromatinolysis existed in FIS mainly. Meanwhile, the apoptotic body and neuron with circular chromatin distributed sporadically. Morphological changes caused by axonal injury and ischemia existed simultaneously at this time. What is responsible for this change? We found obvious glial scars situated around the degenerative neuron. Researchers reported that there are previous studies, which were in support of the point that the glia scar was the key factor to conduce the degeneration of the neuron [16, 17]. This is also due to the fact that the space that is passed by axons was far larger than the neuronal body. The numbers of injured axons were much more than the injured neurons in spinal cord injury. So, the effect of axonal injury on neuronal degeneration should not be neglected. Evidently, neuronal impairment after SCI was caused by different pathogeny and represented at different times and regions. At one week, ischemic change was the main pathologic change while sporadic apoptosis combined after 1 week and gives priority to ischemic change, the morphology change of central chromatinolysis caused by axonal injury appear

in a later point of time and persisted for a long period.

Once neural injury passed through the phase of karyopycnosis, the injured neuron could not be reversed even after removing the injury factor. In our experiment, morphological changes of neuronal karyopycnosis were found at 6 h after injury and presented a chain reaction (inflammatory reaction, low perfusion, and ischemia neural injury). So, the measures aimed at controlling inflammatory reaction should be adopted at the first opportunity to treat secondary neuronal injury. Methylprednisolone, for example, had been adopted and achieved a curative effect [18, 19].

GFAP is a typical skeleton protein uniquely expressed in astrocyte. When ischemia occurred after injury, astrocyte was induced and synthesized GFAP, therefore, it is a biomarker of astrocyte. In our model, the expression of GFAP descended sharply just 1 hour after injury, indicating that there was a visible injury of astrocyte at that time. Approximately 6 hours after injury, glial cell proliferation first appeared in the white matter near the injury region and dorso-spinal cord under the spinal pia mater close to the central canal. What is the reason for this? Researchers detected Nestin expression in adult rat's central canal near the injury region after injury, mainly located in the central canal and proliferated, budded, and migrated in the spinal cord [20], which encouraged us to consider that there had been an endogenous neural stem cell (ENSC) in the spinal cord of the adult rat. ENSC had been activated, generated, and differentiated into astrocyte. Consequently, the astrocyte first appeared at the region where the stem cells exist. 7 days after the injury, the positive expression of GFAP developed from the local region to the hol-region around the injury position. The RC data changed from decrease to enhancement (compared to a normal spinal cord), which implied that under the niche or microenvironment after injury, the astrocyte, which proliferated from stem cells, had persistently migrated to the damaged region. 28 days after the injury, the percentage of astrocyte near the injured region was much higher than that found in a normal spinal cord. Astrocytes gathered mostly in the lesion area and the cell processes of these astrocytes contacted each other and formed into a grid-like structure, surrounded the injured site, and formed the cavity. The relic neurons displayed an islet-like structure around the cavity.

Complications also often occurred after the injury. Mutual mutilation could be avoided by feeding each rat in a separate cage while decreasing the intestinal obstruction through diet, intravenous nutrition, and abdominal massage, thereby reducing mortality. Intestinal obstruction was the leading cause of death (66.67%, n = 6). After the injury, transmission dysfunction and feces accumulated in the intestine lead to mechanical obstruction and further developed to strangulating intestinal obstruction, resulting in death.

Conclusions

A shape-suitable impinger could set up an acute ventral closed SCI model successfully in a simple procedure. Changes in neural function, pathology, and mortality had consistency to the coup momentum. Damage of different degrees could be made by adjustable C.M. This model had distinctive pathological changes, for example, astrocytes underwent acute damage and proliferated in the hyperplasia stage. Neuronal degeneration after SCI was a process consisting of multi-reason, multistage, acute injury, and chronic injury persisting for a long time. A rational therapy aim for neuronal degeneration after SCI needs to adopt corresponding measures based on major pathological contradictions at different times.

Disclosure of conflict of interest

None.

Address correspondence to: Xiaoming Hu, Department of Neurosurgery, Taizhou Hospital of Zhejiang Province Affiliated to Wenzhou Medical University, No. 150 of Ximen Street, Linhai District, Taizhou 317000, China. Tel: +86-0576-85199071; Fax: +86-0576-85199876; E-mail: huxiaoming_qw@163.com; Guanfu Wang, Department of Urinary Surgery, Taizhou Hospital of Zhejiang Province Affiliated to Wenzhou Medical University, No. 150 of Ximen Street, Linhai District, Taizhou 317000, China. Tel: +86-13566339838; Fax: +86-0576-85199876; E-mail: wang8808_dr@163.com

References

[1] Batista CM, Mariano ED, Onuchic F, Dale CS, Dos Santos GB, Cristante AF, Otoch JP, Teixeira

MJ, Morgalla M and Lepski G. Characterization of traumatic spinal cord injury model in relation to neuropathic pain in the rat. Somatosens Mot Res 2019; 36: 14-23.
[2] Thygesen MM, Lauridsen H, Pedersen M, Orlowski D, Mikkelsen TW and Rasmussen MM. A clinically relevant blunt spinal cord injury model in the regeneration competent axolotl (Ambystoma mexicanum) tail. Exp Ther Med 2019; 17: 2322-2328.
[3] Mattucci S, Speidel J, Liu J, Ramer MS, Kwon BK, Tetzlaff W and Oxland TR. Development of a traumatic cervical dislocation spinal cord injury model with residual compression in the rat. J Neurosci Methods 2019; 322: 58-70.
[4] Meng SY, Zhuang XQ, Lu SL, Hu RH, Mo HH and Mo ZG. Pathological changes of ventral acute compressive spinal cord injury model. Chinese Journal of Clinical Rehabilitation 2005; 21: 28-30.
[5] Liu CM, Zhang GL, Wang ZY, Wang CQ, Han CB and Hao XF. A clinical investigation of appropriate sedation depth and dosage of midazolam used as an adjuvent during regional anesthesia. The Journal of Clinical Anesthesiology 2005; 1: 20-22.
[6] Kakulasa BA and Kaelanb C. The neuropathological foundations for the restorative neurology of spinal cord injury. Clin Neurol Neurosurg 2015; 129 Suppl 1: S1-S7.
[7] McBride RL and Feringa ER. Ventral horn motoneurons 10, 20 and 52 weeks after T-9 spinal cord transaction. Brain Res Bull 1992; 28: 57-60.
[8] Emery E, Aldana P, Bunge MB, Puckett W, Srinivasan A, Keane RW, Bethea J and Levi AD. Apoptosis after traumatic human spinal cord injury. J Neurosurg 1998; 89: 911-920.
[9] Schmidt-Kastner R, Flissv H and Hakim AM. Subtle neuronal death in striatum after short forebrain ischmia in rats detected by in situ end-labelling for DNA damage. Stroke 1997; 28: 163-170.
[10] Narang A, Qiao F, Atkinson C, Zhu H, Yang X, Kulik L, Holers VM and Tomlinson S. Natural IgM antibodies that bind neoepitopes exposed as a result of spina cord injury, drive secondary injury by activating complement. J Neuroinflammation 2017; 14: 120.
[11] Fang Y, Huang X, Wan Y, Tian H, Tian Y and Wang W. Deficiency of TREK-1 potassium channel exacerbates secondary injuryfollowing spinal cord injury in mice. J Neurochem 2017; 141: 236-246.
[12] Wang J, Chen J, Jin H, Lin D, Chen Y, Chen X, Wang B, Hu S, Wu Y, Wu Y, Zhou Y, Tian N, Gao W, Wang X and Zhang X. BRD4 inhibition attenuates inflammatory response in microglia and facilitates recovery after spinal cord injury in rats. J Cell Mol Med 2019; 23: 3214-3223.
[13] Bisicchia E, Latini L, Cavallucci V, Sasso V, Nicolin V, Molinari M, D'Amelio M and Viscomi MT. Autophagy inhibition favors survival of rubrospinal neurons after spinal cord hemisection. Mol Neurobiol 2017; 54: 4896-4907.
[14] Dai W, Wang X, Teng H, Li C, Wang B and Wang J. Celastrol inhibits microglial pyroptosis and attenuates inflammatory reactionin acute spinal cord injury rats. Int Immunopharmacol 2019; 66: 215-223.
[15] Hassannejad Z, Zadegan SA, Vaccaro AR, Rahimi-Movaghar V and Sabzevari O. Biofunctionalized peptide-based hydrogel as an injectable scaffold for BDNF delivery can improve regeneration after spinal cord injury. Injury 2019; 50: 278-285.
[16] Wang SM, Hsu JC, Ko CY, Chiu NE, Kan WM, Lai MD and Wang JM. Astrocytic CCAAT/enhancer-binding protein delta contributes to glial scar-formation and impairs functional recovery after spinal cord injury. Mol Neurobiol 2016; 53: 5912-5927.
[17] Kumar H, Choi H, Jo MJ, Joshi HP, Muttigi M, Bonanomi D, Kim SB, Ban E, Kim A, Lee SH, Kim KT, Sohn S, Zeng X and Han I. Neutrophil elastase inhibition effectively rescued angiopoietin-1 decrease and inhibits glial scar after spinal cord injury. Acta Neuropathol Commun 2018; 6: 73.
[18] Manley NC, Priest CA, Denham J, Wirth ED and Lebkowski JS. Human embryonic stem cell-derived oligodendrocyte progenitor cells: preclinical efficacy and safety in cervical spinal cord injury. Stem Cells Transl Med 2017; 6: 1917-1929.
[19] Suberviola B, González-Castro A, Llorca J, Ortiz-Melón F and Miñambres E. Early complications of high-dose methylprednisolone in acute spinal cord injury patients. Injury 2008; 39: 748-752.
[20] Gao YL and Feng Y. Change of neural stem cell and its derived support factor give in big rat after spinal cord injury. Journal of Clinical Rehabilitative Tissue Engineering Research 2007; 12: 10066-10069.